Engineering in Life Sciences

WILEY-VCH

Engineering in Life Sciences

RESEARCH ARTICLE OPEN ACCESS

Combination of Two-Stage Continuous Feeding and Optimized Synthetic Medium Increases Lipid Production in *Lipomyces starkeyi*

Chih-Chan Wu[1] | Kenji Okano[1,2] | Pijar Religia[1] | Yuki Soma[3] | Masatomo Takahashi[4] | Yoshihiro Izumi[4] | Takeshi Bamba[4] | Kohsuke Honda[1,5]

[1]International Center for Biotechnology, Osaka University, Suita, Osaka, Japan | [2]Department of Life Science and Biotechnology, Faculty of Chemistry, Materials and Bioengineering, Kansai University, Suita, Osaka, Japan | [3]Synthetic Bioengineering Research Group, Bioproduction Research Institute, National Institute of Advanced Industrial Science and Technology, Tsukuba, Ibaraki, Japan | [4]Division of Metabolomics/Mass Spectrometry Center, Medical Research Center for High Depth Omics, Medical Institute of Bioregulation, Kyushu University, Fukuoka, Japan | [5]Industrial Biotechnology Initiative Division, Institute for Open and Transdisciplinary Research Initiatives, Osaka University, Suita, Osaka, Japan

Correspondence: Kohsuke Honda (honda.kohsuke.icb@osaka-u.ac.jp)

Received: 15 July 2024 | **Revised:** 12 November 2024 | **Accepted:** 15 January 2025

Funding: This research was supported by the NEDO Project (project code: P20011) of the Ministry of Economy, Trade, and Industry (METI), Japan.

Keywords: fermentation | high cell density | *Lipomyces starkeyi* | microbial lipid | oleaginous yeast | synthetic medium

ABSTRACT

The oleaginous yeast *Lipomyces starkeyi* is recognized for its remarkable lipid accumulation under nitrogen-limited conditions. However, precise control of microbial lipid production in *L. starkeyi* remains challenging due to the complexity of nutrient media. We developed a two-stage fed-batch fermentation process using a well-defined synthetic medium in a 5-L bioreactor. In the first stage, the specific growth rate was maintained at a designated level by maximizing the cell density through optimizing the feeding rate, molar carbon-to-nitrogen (C/N) ratio, and phosphate concentration in feeding media, achieving a high cell density of $213 \pm 10 \times 10^7$ cells mL^{-1}. In the second stage, we optimized the molar C/N ratio in the feeding medium for lipid production and achieved high biomass (130 ± 5 g L^{-1}), lipid titer (88 ± 6 g L^{-1}), and lipid content (67% ± 2% of dry cellular weight). Our approach yielded a high lipid titer, comparable to the highest reported value of 68 g L^{-1} achieved in a nutrient medium, by optimizing cultivation conditions with a synthetic medium in *L. starkeyi*. This highlights the importance of well-established yet powerful bioprocess approaches for the precise control of microbial cultivation.

1 | Introduction

Triacylglycerols (TAG), a type of microbial lipids, are considered sustainable alternatives for replacing non-renewable petroleum and plant-derived oils in industries such as biofuels, food, pharmaceuticals, and cosmetics [1–3]. Oleaginous yeasts have garnered significant attention due to their outstanding lipid-producing abilities under specific culture conditions [4]. One such oleaginous yeast, *Lipomyces starkeyi*, has recently gained substantial recognition for its remarkable oleaginicity, capable of accumulating lipid content up to 85% of dry cellular weight (DCW) [5]. Additionally, this yeast has exhibited good tolerance to fermentation inhibitors, such as furfural and its derivatives, and low-pH conditions [6, 7] and can also utilize a variety of low-cost carbon sources, including lignocellulosic biomass, starchy materials, and biodiesel-derived glycerol for lipid production [8–11]. Recent advancements, including the publication and establishment of the whole-genome sequence, metabolic mod-

Summary

- A bioprocess for lipid production was established using a synthetic medium.
- Cell growth and lipid accumulation could be separated by controlling the C/N ratio.
- Depletion of phosphate and nitrogen triggers the lipid accumulation.
- Supplement of nitrogen sustained cell number during lipid production.

ules, and gene manipulation methods, have further expanded the possibilities for genetic manipulation aimed at enhancing lipid production [8, 12–15]. Therefore, the remarkable lipid-producing ability of *L. starkeyi*, coupled with the availability of cellular information and molecular genetic tools, makes this yeast a potential chassis for various industrial applications.

Nitrogen limitation is one of the well-studied inducing factors that trigger lipid accumulation in oleaginous yeasts. When the nitrogen source is depleted in the growth media, excessive carbon sources are used for lipid synthesis [13]. Numerous attempts have been made to increase lipid production in oleaginous *L. starkeyi* by optimizing the molar carbon-to-nitrogen (C/N) ratio in nutrient media [9, 15–18]. These nutrient media were often supplemented with complex ingredients such as yeast extract or peptone, which contain amino acids, vitamins, or nucleic acid components [9, 15–18]. Lin et al. [17] found that the cell propagation of *L. starkeyi* was almost completely inhibited, and lipids accumulated in cells when nitrogen was deprived in the glucose solution. Hence, Lin et al. [17] developed a two-stage fermentation process for lipid production in *L. starkeyi*. The group first cultured the *L. starkeyi* in 10 L of nutrient-rich YEPD (yeast extract/peptone/glucose) medium in a 15-L bioreactor to maximize cell density. Subsequently, all cells were harvested and transferred into a 10-L bioreactor containing 4 L of 120 g L^{-1} glucose solution. By employing the two-stage fermentation method, Lin et al. [17] successfully obtained a remarkable dry cell weight (DCW) of 105 g L^{-1}, a lipid titer of 68 g L^{-1}, and a lipid content of 65% of DCW in *L. starkeyi*. Although high lipid titers and contents with nutrient media have been achieved, precisely controlling lipid accumulation during cultivation by the use of complex ingredients is difficult due to variability in nutrient sources caused by the difference in the production area, seasons, and processing methods of raw materials. Additionally, the bioprocess of transferring biomass from one vessel to another may lead to contamination and difficulties when scaling up to an industrial level. To address these issues, developing a simple and predictable lipid production strategy is important and urgent for harnessing *L. starkeyi* for industrial applications.

A chemically defined synthetic medium allows for precise and controllable formulation, ensuring comparable and repeatable results during microbial cultivation [19]. Moreover, employing a synthetic medium for microbial cultivations offers several advantages, including cost savings on substrates, simplification of downstream purification processes, and reduced risk of contamination [20]. Attempts have been made to explore the lipid-producing ability of *L. starkeyi* using synthetic media in flask-scale trials, and high lipid contents has been achieved [5, 7, 21, 22]. However, the maximum lipid titers achieved using synthetic media have not been on par with those attained using nutrient-rich media [17]. For example, Juanssilfero et al. [5] demonstrated that using a synthetic medium with xylose and glucose as carbon sources yielded a high lipid content of 87%, but the lipid titer reached only 22 g L^{-1}. One reason for the lower lipid titer using synthetic media could be attributed to poor cell density. Fed-batch culture with constant feeding rates or pulsed feeding strategies is a popular and well-established feeding mode for cultivating various microorganisms [23–26]. However, both strategies can lead to substrate accumulation or insufficient nutrient supply, which may curtail the growth phase and limit cell density in the bioreactor [27]. To achieve efficient and economically feasible lipid production, rapid cell propagation at the highest growth rate is essential to shorten cultivation time and reduce production costs. To address the issue of low cell density when using synthetic media, we developed a two-stage fed-batch fermentation process comprising a growth phase and a lipid production phase (Figure 1). First, an exponential feeding strategy was employed with nitrogen-rich synthetic media to maximize the cell density. Second, a constant feeding strategy was applied with nitrogen-limited synthetic media. Additionally, we optimized nutrient consumption of feeding media during the two phases of fed-batch fermentation. Eventually, we achieved high lipid titers and contents, which are comparable to those in previous studies using nutrient-rich media. Furthermore, the fatty acid profiles of the obtained lipids closely resembled those of plant-derived oils. This study presents a conventional yet strategically designed procedure that highlights the rational optimization of cultivation conditions in a fermentation process utilizing a controllable synthetic medium for the microbial production of lipids and other valuable metabolites.

2 | Materials and Methods

2.1 | Yeast Strain, Culture Media, and Cultivation

The yeast strain *L. starkeyi* NBRC10381, obtained from the National Bioresource Research Center, NITE (Chiba, Japan), was used throughout this study. This strain was grown in yeast extract/peptone/glucose broth (YPD) (20 g L^{-1} glucose, 10 g L^{-1} yeast extract, and 10 g L^{-1} peptone) at 30°C for 48 h. The culture was then mixed with the same volume of sterilized 300 g L^{-1} glycerol solution and stored at −80°C as seed stock for the following experiments. The pre-culture medium (30 g L^{-1} glucose, 5 g L^{-1} $(NH_4)_2SO_4$, 1 g L^{-1} KH_2PO_4, 0.1 g L^{-1} NaCl, 1 g L^{-1} yeast extract, 0.5 g L^{-1} $MgSO_4 \cdot 7H_2O$, and 0.1 g L^{-1} $CaCl_2 \cdot 2H_2O$; pH 5.5) [28] was used for the cell pre-culture. The pre-cultivation was performed in a reciprocal shaker at 140 stoke per minute and 30°C for 72 h.

In addition to providing carbon, nitrogen, vitamins and trace elements are necessary for cell growth and metabolite production [21]. A synthetic medium was used as the basic fermentation medium in this study [21]. The synthetic medium was prepared by mixing sterile glucose solution (working concentration: 20 g L^{-1} glucose), a salt solution (working concentrations: 1.5 g L^{-1} KH_2PO_4, 1.5 g L^{-1} KCl, 0.5 g L^{-1} $MgSO_4 \cdot 7H_2O$), vitamin mixtures

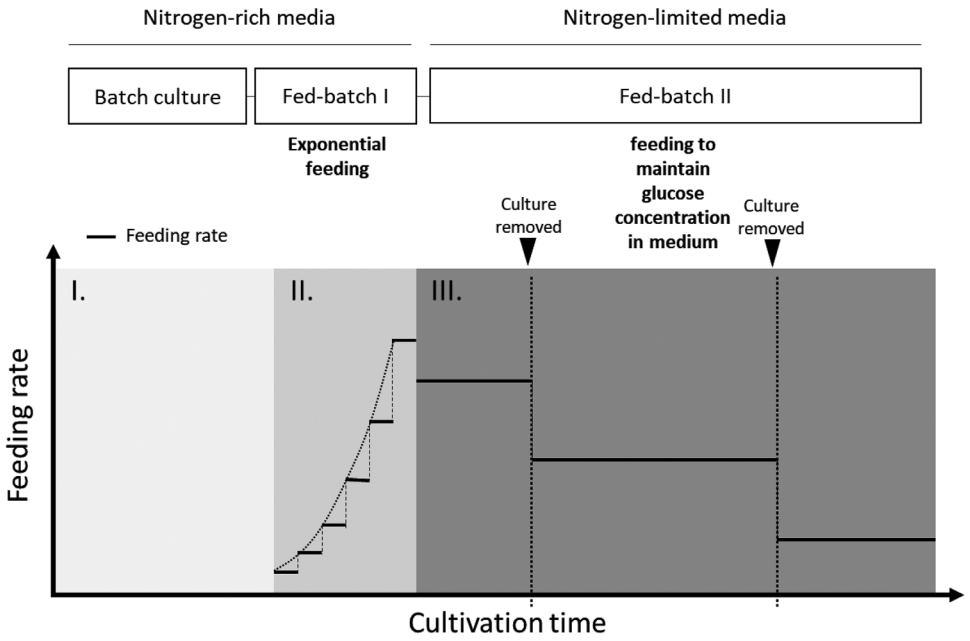

FIGURE 1 | Cultivation stages and feeding strategies in this study. The cultivation processes were separated into three parts. I. Batch culture phase. II. Fed-batch with exponential feeding phase. III. Fed-batch with constant feeding phase. Due to the removal of culture during this phase, the feeding rate was decreased accordingly to maintain the glucose concentration in the medium.

(working concentrations: 1 mg L^{-1} each of biotin, pyridoxine, thiamine, riboflavin, *para*-aminobenzoic acid, and nicotinic acid), and a trace element solution (working concentrations: 2.25 mg L^{-1} $ZnSO_4 \cdot 7H_2O$, 11 mg L^{-1} H_3BO_3, 5 mg L^{-1} $MnCl_2 \cdot 4H_2O$, 5 mg L^{-1} $FeSO_4 \cdot 7H_2O$, 1.7 mg L^{-1} $CoCl_2 \cdot 6H_2O$, 1.6 mg L^{-1} $CuSO_4 \cdot 5H_2O$, 0.085 mg L^{-1} $Na_2MoO_4 \cdot 2H_2O$, and 5 mg L^{-1} Na_4EDTA). The desired molar C/N ratio of the medium was adjusted by mixing the synthetic medium with a sterile NH_4Cl solution.

2.2 | Fermentation

The fermentation process was divided into two stages (cell propagation and lipid production). For the cell propagation stage, a batch culture was performed to acquire primary biomass using a synthetic medium. To start the batch cultivation, the pre-cultured cells in nutrient medium were collected and washed once with distilled water. The cells were then inoculated into the culture medium in a 5-L stirred tank reactor (BML-05NP4) (ABLE and Biott, Tokyo, Japan) to a cell density of 1×10^6 cells mL^{-1} to start the cultivation. The initial volume of the culture was 2 L. The temperature was controlled at 30°C, and the pH was maintained at 5.5 by the addition of 5 N NaOH solution. Agitation and aeration were set at 100 rpm and 2 L mL^{-1}, respectively, at the beginning of fermentation. Afterward, the agitation was controlled from 100 to 1100 rpm to keep the dissolved oxygen (DO) at 50% (100% of saturated oxygen levels at 30°C) in the culture media using an automatic control system (ABLE and Biott). The aeration was manually changed from 2 to 4 L mL^{-1} when the maximum agitation was reached to prevent the depletion of DO to 0%. Antifoam LG109 (Adeka, Tokyo, Japan) was added as needed to minimize foaming. After exhaustion of glucose, fed-batch culture with an exponential feeding strategy was carried out to maintain a designated level of the specific growth rate (a μ-stat growth) of the cells. A 0.5 L of feeding medium containing 500 g L^{-1} glucose in the synthetic medium was used during the fed-batch culture. In the exponential feeding strategy (with the same molar C/N ratio of 7.1 in batch culture), the concentrations of KH_2PO_4 (3 g L^{-1}), $MgSO_4 \cdot 7H_2O$ (1 g L^{-1}), and KCl (1 g L^{-1}) were doubled in the initial batch cultures and feeding media to prevent deficiencies in essential nutrients such as phosphate, sulfate, and Mg^{2+} and K^+, which play crucial roles in cellular physiology [29, 30]. The feeding medium was sterilized using a 0.22-μm filter before being introduced into the fermenter.

For the lipid production stage, a fed-batch cultivation with a constant feeding rate began once the glucose in the culture was exhausted. A 3-L nitrogen-limited feeding medium (containing 500 g L^{-1} of glucose in the synthetic medium) was fed at a feeding rate of 50 mL h^{-1} at the beginning and gradually decreased with stepwise manner to maintain the residual glucose lower than 20 g L^{-1} in the culture. At approximately 3-L culture volume, 1.5 L of culture was removed to prevent broth spillage by increasing tank pressure (demonstrated in Supplementary Data 1).

2.3 | Analytical Methods

At each sampling time point, 10 mL of culture was collected for the measurement of various parameters, including cell density, DCW, glucose concentration, nitrogen and phosphate levels, lipid titer and content, and fatty acid composition. Cell density was determined by counting the number of cells in a diluted culture using a hemocytometer (117-112C; Watson, Hyogo, Japan) under a bright-field microscope. The sampled cultures were then centrifuged at 8000 × *g* for 5 min at 4°C to separate the supernatant from the cell pellets. The cell pellets were washed once with distilled water and subsequently lyophilized until a constant weight was achieved, allowing for gravimetric determination of DCW. The supernatants were preserved at −20°C

for further analysis. Glucose concentration in the supernatant was determined using a biosensor BF-9 with a glucose electrode (Oji Scientific Instruments, Hyogo, Japan). Inorganic nitrogen (NH_4-N) and phosphate (PO_4-P) levels in the culture broth from the samples were quantified using commercial kits: LabAssay Ammonia (Fujifilm Wako Pure Chemicals, Osaka, Japan) for nitrogen and the Malachite Green Phosphate Assay Kit (BioAssay Systems, CA, USA) for phosphate.

2.4 | Specific Growth Rate and Yield Calculation

The specific growth rate (μ, h^{-1}) and biomass yield ($Y_{X/S}$, g g^{-1}) were calculated using the DCW (X_{DCW}, g) and glucose (S, g) of samples withdrawn at different time points, according to the following Equations (1) and (2):

$$\mu = \left(\frac{1}{X_{DCW}}\right)\left(\frac{dX_{DCW}}{dt}\right) = \frac{d\left(\ln X_{DCW}\right)}{dt} \quad (1)$$

$$Y_{X/S} = \frac{\Delta\left(X_{DCW}\right)}{\Delta\left(s\right)} \quad (2)$$

where t represents the time of each sampling point (h).

2.5 | Exponential Feeding Profile

An exponential feeding strategy was applied for the μ-stat fed-batch cultivation to achieve a μ-stat growth of the cells using glucose as a restriction substrate. A 0.5-L feeding medium containing 500 g L^{-1} glucose was fed from the end of batch culture (see Figure 1) with gradually increased exponential feeding rates (F) calculated according to the following Equation (3) [31]:

$$F = \frac{\mu_{set} V_0 X_0 \exp\left(\mu_{set} t\right)}{Y_{X/S(set)} S_F} \quad (3)$$

where μ_{set} is the target μ (h^{-1}), $Y_{X/S(set)}$ is the target $Y_{X/S}$ (g g^{-1}), V_0 and X_0 are the initial volumes of medium in fermenter (L) and DCW (g L^{-1}) at the starting time 0 h, respectively, S_F is the concentration of glucose in feeding medium, and t is the time difference between the feeding point and the feeding starting point. The predetermined μ_{set} and $Y_{X/S(set)}$ were set to determine the feeding rate.

2.6 | TAG Quantification and Fatty Acid Analysis

A method for quantifying lipids (TAG) was modified and adapted to determine the lipid content [28]. In brief, dried yeast pellets (10–50 mg) were suspended in distilled water and homogenized with 1 g of 0.5-mm glass beads (YGB05, Oji Scientific Instruments). The lipid content was quantified using a commercial kit, LabAssay Triglyceride (Fujifilm Wako Pure Chemicals). Fatty acid profiles were determined through gas chromatography analysis. Lipids were extracted and subsequently converted into fatty acid methyl esters (FAME) using the same commercial kit, the Fatty Acid Methylation Kit (Nacalai Tesque, Kyoto, Japan), for gas chromatography analysis. Lipid samples are taken at the end of cultivation time for each different condition (Nitrogen-free = 192 h, C/N ratio 200 = 168 h, C/N ratio 400 = 168 h). Heptadecanoic acid (C17) was added to the samples during lipid extraction and used as an internal standard for FAME quantification. The FAME samples were analyzed using a GC-2014 gas chromatograph (Shimadzu, Kyoto, Japan) equipped with a flame ionization detector (FID) and a capillary column DB-FATWAX UI (Agilent Technologies, CA, USA). Nitrogen gas was employed as the carrier gas with a constant linear velocity of 50 cm s^{-1}. The column temperature was programmed to start at 120°C and maintained for 1 min, and then increased to 180°C at a rate of 20°C min^{-1}, and held for 10 min. Subsequently, the temperature was raised to 220°C at a rate of 5°C min^{-1} and held for 5 min. Individual FAMEs were identified by comparing sample retention times with a commercial FAME standard, Supelco 37 Component FAME Mix (Sigma-Aldrich, MO, USA), and quantified by comparison with the internal standard.

2.7 | Lipid Yield Calculation

To determine the final lipid yield of the fed-batch culture, total lipid amount (P), including removed culture and consumed glucose (S) throughout the cultivation process, was measured. Lipid yield ($Y_{L/S}$, lipid-g/glucose-g) was calculated according to Equation (4):

$$Y_{L/S} = \frac{\Delta\left(P\right)}{\Delta\left(S\right)} \quad (4)$$

where $\Delta(P)$ and $\Delta(S)$ indicate differences in the produced lipid and consumed glucose, respectively, at the sampling point and the starting point of cultivation.

2.8 | Statistical Analysis

Statistical analysis was performed using R software, version 3.4.1, with one-way analysis of variance (ANOVA) and Tukey's post hoc test. We performed the analysis to examine the significance of differences in data from different time points and treatments, as shown in Figures 2–6. We do not show the significant difference on figures because of too many data points; hence, we highlighted the significance in Section 3.

3 | Results and Discussion

3.1 | C/N Ratio of 7.1 Gives Highest Cell Growth in Batch Cultivation

To date, no studies that applied synthetic media for lipid production in *L. starkeyi* have succeeded in achieving lipid titers comparable to those achieved with nutrient media, primarily due to low cell densities [8, 17]. To establish a platform for high lipid titer production using a synthetic medium, we attempted to employ a two-stage fed-batch fermentation strategy consisting of a cell growth phase and a lipid accumulation phase. In the growth phase, we aimed to maximize cell density using an exponential feeding strategy to maintain a high growth rate. To optimize the molar C/N ratio for cell growth and determine the suitable ranges of specific growth rate (μ, h^{-1}) and biomass

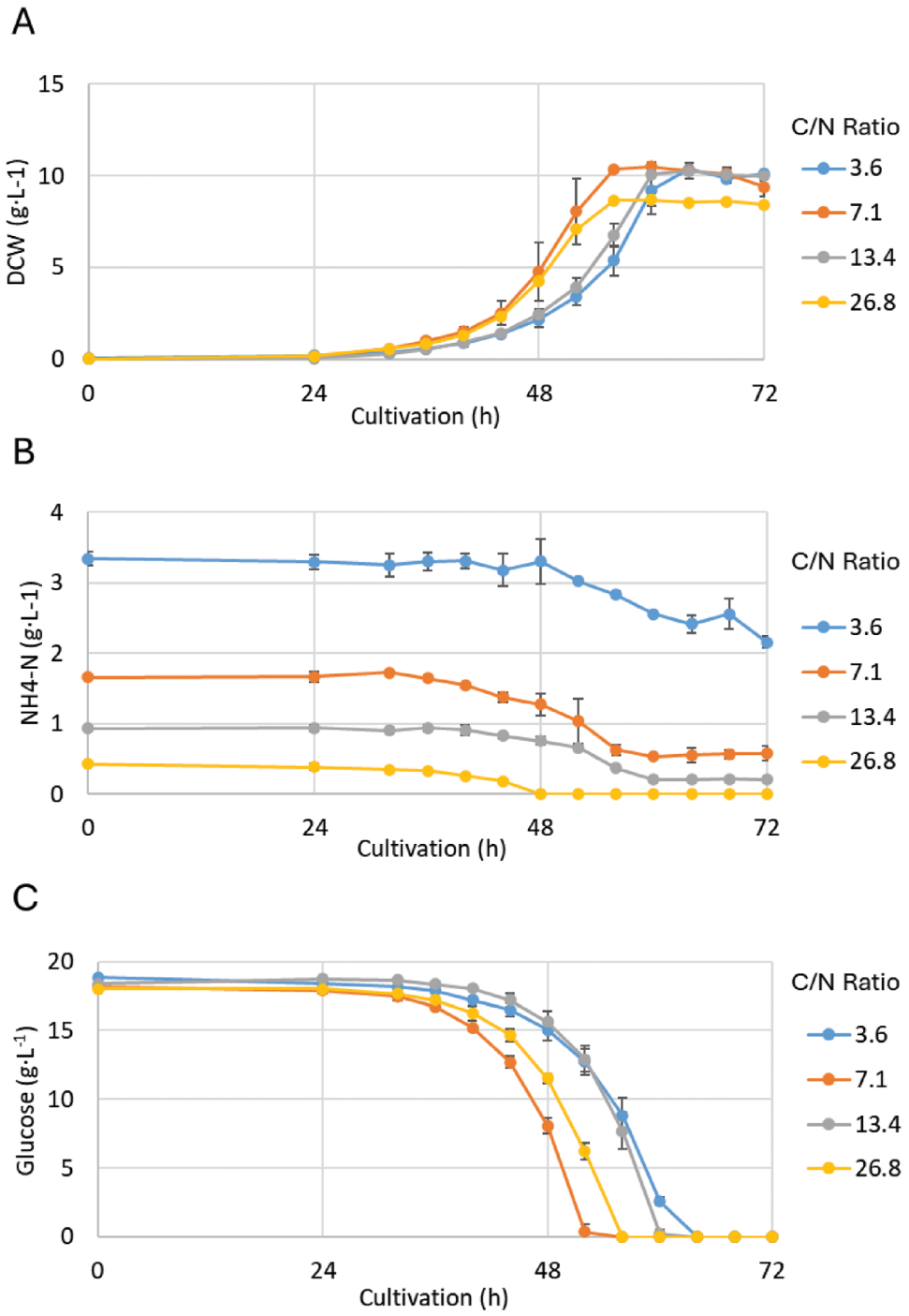

FIGURE 2 | Effect of different molar C/N ratios on the biomass concentration. Batch cultures with various C/N ratios in the culture media were performed. The glucose concentration in the culture media was 20 g L^{-1}. The cultures were monitored for 72 h. Dry biomass (A), residual ammonia (NH_4-N) (B), and glucose (C) in the culture media were measured at each time point. All experiments were carried out in parallel triplicates. Data are presented as mean ± standard deviation.

yield ($Y_{X/S}$, g g^{-1}) for calculation in exponential feeding rate in Equation (3), we cultivated yeast cells in the synthetic media with various molar C/N ratios by adjusting the amount of nitrogen (NH_4Cl) in media containing 20 g L^{-1} of glucose. The growth and substrate consumption kinetics of batch cultivations are presented in Figure 2. The results indicate that a low molar C/N ratio (3.6), which contained the highest nitrogen among the assessed conditions, led to a lower growth rate (Figure 2A). In contrast, a high molar C/N ratio (26.8), which contained the lowest nitrogen among the assessed conditions, resulted in the lowest biomass due to insufficient residual ammonia in the culture broth (Figure 2B). These data suggest that the ammonia concentration in media affected cell growth. In addition, although the glucose concentrations were at the same levels at the starting time of each cultivation, different C/N ratios in the media also affected the glucose consumption for cell growth (Figure 2C). Although final concentration of biomass converged at a similar level in tested conditions, the highest dry cells weight (11 g L^{-1})

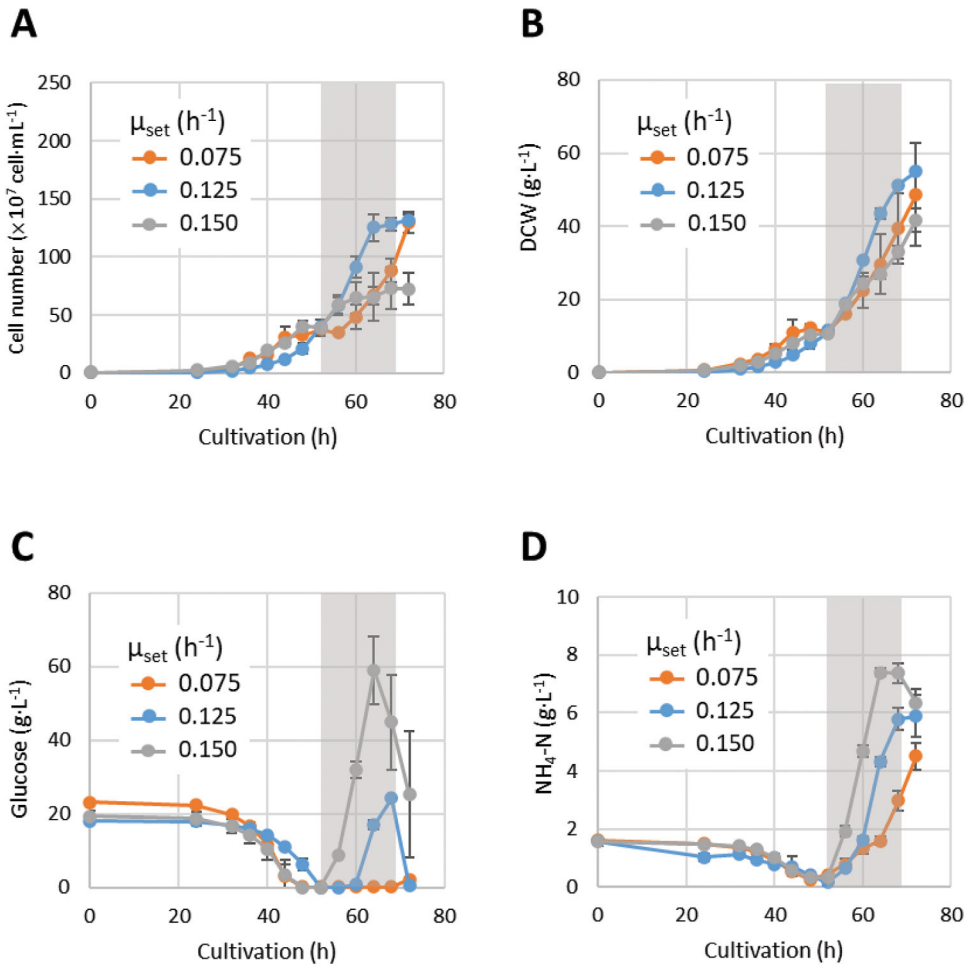

FIGURE 3 | Optimization of feeding rate in the fed-batch culture with exponential feeding mode. Feeding patterns (μ_{set}: 0.075, 0.125, and 0.150 h; $Y_{X/S(set)}$: 0.45 g g^{-1}) were predetermined according to Equation (3) (Section 2.4). Exponential feeding with various feeding patterns began at 52 h and continued until 0.5 L of feeding media were consumed. The glucose concentration in the feeding media was 500 g L^{-1}. The gray areas in the figure indicate the feeding periods. The cultures were monitored for 72 h, and measurements included cell number (A), DCW (B), residual glucose (C), and ammonia (NH_4-N) (D) in the culture media at each time point. All experiments were conducted in triplicate, and the data are presented as mean ± standard deviation.

was achieved with C/N ratio of 7.1 in the shortest cultivation time of 56 h (ANOVA, Tukey's honestly significant difference, $p < 0.05$; Figure 2A). During the log phase of molar C/N ratio equal to 7.1, the specific growth rate (μ, h^{-1}) and biomass yield ($Y_{X/S}$, g g^{-1}) ranged from 0.10 to 0.14 h and from 0.45 to 0.58, respectively. Therefore, the ranges of specific growth rate and yield coefficients were used to calculate the exponential feeding rate for exponential feeding strategies.

3.2 | C/N Ratio of 16 and 6 g L^{-1} Phosphate in Exponential Feeding Conditions Give Highest Cell Density

To achieve a high cell density of *L. starkeyi* during the growth phase, we applied an exponential feeding method (Section 2.4). Based on the data in Figure 2, the yield ($Y_{X/S}$, g g^{-1}) during the log phase ranged from 0.45 to 0.58 g g^{-1}, and the growth rate (μ) ranged from 0.10 to 0.14 h. Accordingly, fed-batch cultivations were performed with three predetermined exponential feeding patterns (μ_{set}: 0.075, 0.125, and 0.150 h) while $Y_{X/S(set)}$ was fixed at 0.45 g g^{-1}, which would generate low (μ_{set}: 0.075 h), middle (μ_{set}: 0.125 h), and high (μ_{set}: 0.150 h) feeding conditions for cell propagation.

As shown in Figure 3A,B, cell density and DCW reached the highest values of 132 ± 4 × 10^7 cells mL^{-1} and 55 ± 2 g L^{-1}, respectively, when the feeding pattern was set with μ_{set} equal to 0.125 and $Y_{X/S(set)}$ equal to 0.45 g g^{-1}. Although cell density increased from 40 ± 6 × 10^7 cells mL^{-1} at 52 h to 132 ± 4 × 10^7 cells mL^{-1} at 72 h, cell proliferation ceased from 64 to 72 h during feeding. We confirmed that the dissolved oxygen level remained sufficient (data not shown), while glucose and nitrogen drastically accumulated at the end of exponential feeding (Figure 3C,D), particularly when the feeding rates are 0.125 and 0.150 h. The glucose level of 0.075-h feeding rate was not accumulated, probably due to the low feeding rate of glucose, at which cell growth and glucose consumption were balanced. From these observations, we considered cell growth was inhibited by the accumulated substrates, particularly NH_4-N. According to our previous results (Figure 2), high concentration of NH_4-N up to 3.3 g L^{-1} inhibited the cell growth. Hence, we optimized the molar

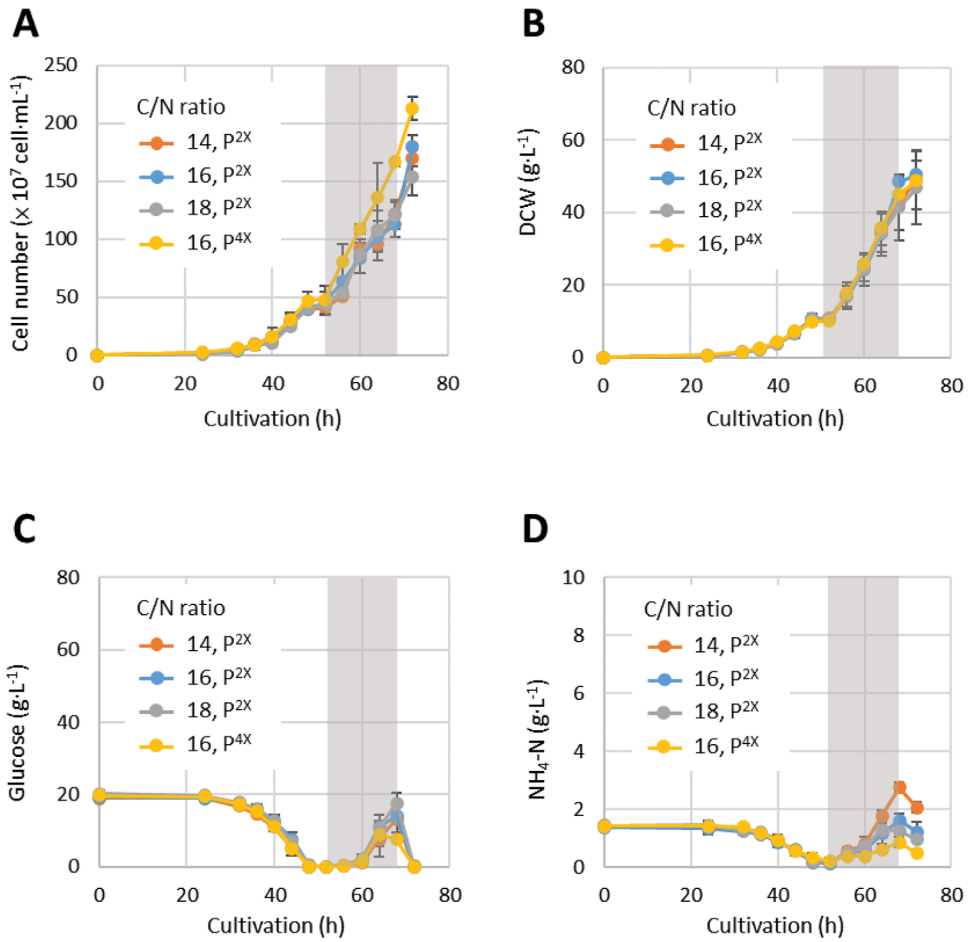

FIGURE 4 | Optimization of the molar C/N ratio and phosphate concentration in feeding media on the fed-batch culture with exponential feeding. Synthetic media with various molar C/N ratios (14, 16, and 18) and 3 or 6 g L^{-1} of KH_2PO_4 (denoted as P^{2X} and P^{4X}) were fed. The glucose concentration in the feeding media was 500 g L^{-1}. The feeding pattern (μ_{set}: 0.125 h; $Y_{X/S}$: 0.45 g g^{-1}) was predetermined according to Equation (3) (Section 2.4). Exponential feeding began from 52 to 68 h. Gray areas indicate the feeding periods. The cultures were monitored for 72 h. Cell number (A), DCW (B), residual glucose (C), and ammonia (NH_4-N) (D) in the culture media were measured at each time point. All experiments were carried out in triplicate. Data are presented as mean ± standard deviation.

C/N ratio of feeding media by calculating new C/N ratio from glucose and ammonia consumption during fermentation from the previous data (Figure 3C, D, calculation not shown). Based on this calculation, we got an average C/N ratio of 16, leading to the predetermined C/N ratios of 14, 16, and 18 for the next set of experiments. Using this new C/N ratios, the cell density was increased from 132 ± 4 × 10^7 cells mL^{-1} (Figure 3A) to 179 ± 10 × 10^7 cells mL^{-1} (Figure 4A) when the C/N ratio is 16 in the feeding media. Previously, the inhibition of cell growth was observed from 64 to 68 h (Figure 3A) along with a substrate accumulation (Figure 3C,D). By increasing the C/N ratio to 16, we were able to cease this inhibition (Figure 4A). Continuous increase in DCW was also observed despite increasing the C/N ratio to 16 or not (Figures 3B and 4B). Furthermore, cells with intracellular lipid droplets were visible under the microscope (data not shown), indicating cultivation phase was shifted from the cell growth to lipid production phase, despite the presence of high concentration of nitrogen. Previous studies have shown that not only nitrogen starvation but also phosphate starvation can induce lipid accumulation in oleaginous yeast [32]. Furthermore, phosphorus (P), mainly incorporated into nucleic acids, phospholipids, and coenzymes, is one of the essential elements for cell growth [32]. Therefore, we suspected that the cessation of cell growth with visible lipid droplets in *L. starkeyi* cells might result from an insufficient phosphorus supply from the media. By measuring the residual phosphate (PO_4-P) concentration during exponential feeding, we found that the phosphate concentration gradually decreased to 0 g L^{-1} at 68 h when initially supplied at 3 g L^{-1} (Figure S2). With the condition of C/N ratio of 16 and phosphate of 3 g L^{-1}, we reached high cell density of 179.4 ± 10 × 10^7 cells mL^{-1} (Figure 4A). Therefore, we further increased the concentration of KH_2PO_4 from 3 to 6 g L^{-1} in the feeding media with the same C/N ratio of 16 to verify our hypothesis that insufficient phosphorus supply hinders the cell growth. By supplementing the phosphate source, the cell density further increased to 213 ± 10 × 10^7 cells mL^{-1} (Figure 4A), which was 1.6 times higher than the previous density of 132 ± 4 × 10^7 cells mL^{-1} (Figure 3A) before optimization. In summary, based on the data from Figure S2 and Figure 4, cell density could be further elevated by reducing substrate accumulation and supplementing phosphate concentration during exponential feeding. The present data also highlight the importance of phosphate in cell growth, as well as in the induction of lipid accumulation, in *L. starkeyi*.

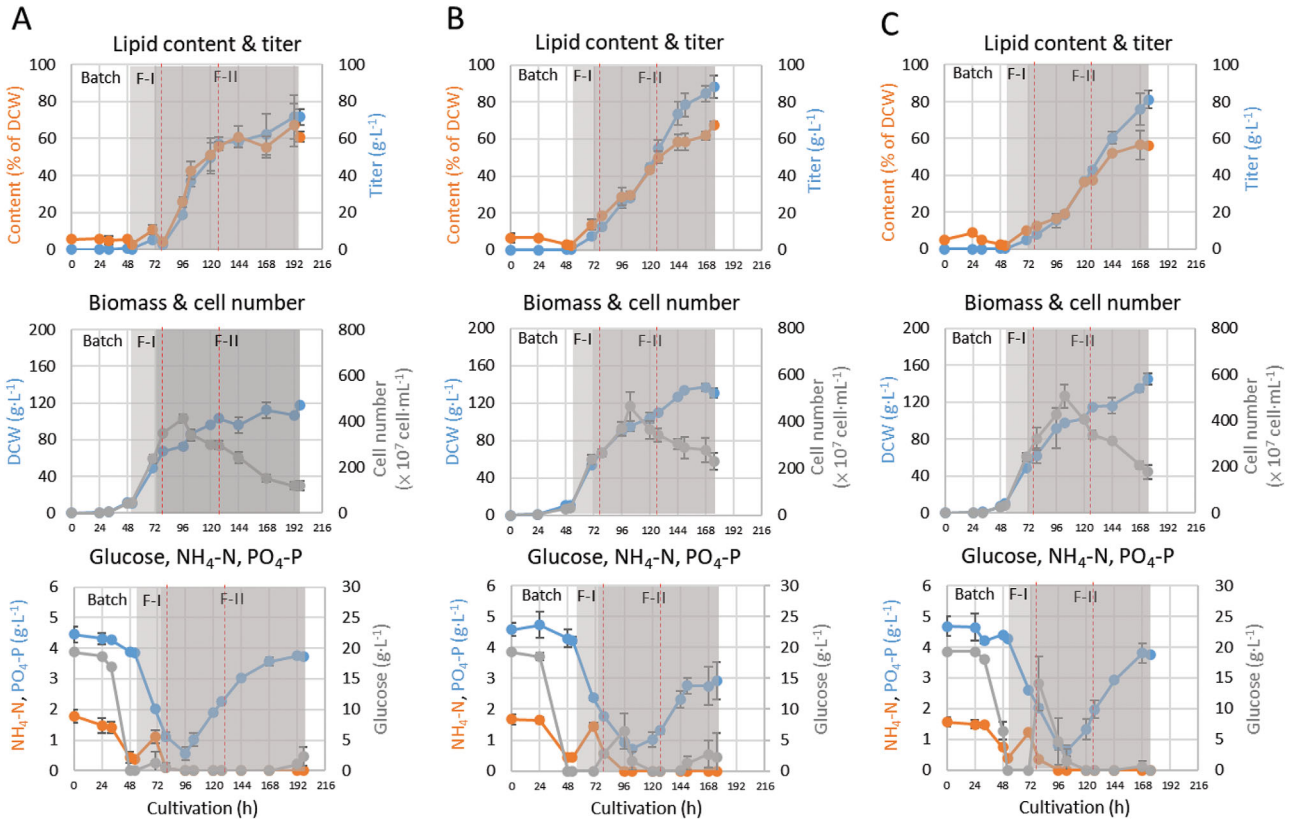

FIGURE 5 | Effects of different molar C/N ratios in feeding media on biomass concentration and lipid production in the fed-batch culture with constant feeding. The synthetic medium without nitrogen (A) and those with molar C/N ratios of 200 (B) and 400 (C) were fed during the lipid production phase. The glucose concentration in the feeding media was 500 g L^{-1}. Three liters of nitrogen-limited media (nitrogen-free and C/N equal to 200 or 400) were fed starting at 70 h after the exponential feeding phase. The feeding rate was set at 50 mL h^{-1} and gradually decreased to prevent the residual glucose concentration from exceeding 20 g L^{-1}. Light gray areas indicate the fed-batch I, while dark gray areas indicate the fed-batch II periods. The cultures were monitored until 3 L of feeding medium was exhausted. To prevent spillage, 1.5 L of culture broth was removed twice when the culture volume reached around 3 L. Red dashed lines indicate the time points of removing culture broths. The cultures were monitored until the 3-L feeding media were depleted. Cell number, DCW, residual glucose, ammonia (NH_4-N), and phosphate (PO_4-P) in the culture media were measured at each time point. All experiments were carried out in triplicate. Data are presented as mean ± standard deviation.

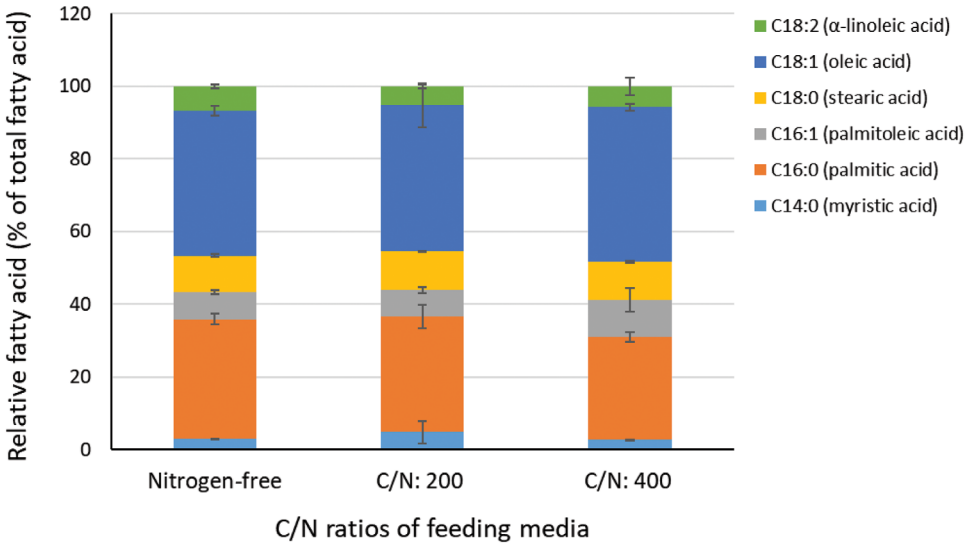

FIGURE 6 | Fatty acid profiles of produced lipids in *Lipomyces starkeyi* NBRC10381 cultured with different molar C/N ratios. Samples were collected at the end of the cultivations. Lipid and fatty acid ester mixtures were extracted and prepared as mentioned in Section 2.6. All experiments were carried out in parallel triplicates. Data are presented as mean ± standard deviation.

3.3 | Two-Stage Continuous Feeding With Limited Nitrogen Media Gives High Lipid Titer

Nitrogen starvation is a well-studied method to induce lipid accumulation in oleaginous yeasts. When the nitrogen source is depleted in the growth media, excessive carbon sources are used for lipid synthesis [13]. Studies [33, 34] have discussed that an efficient way to maximize lipid productivity in whole cell biocatalysts is separating the phases of cell propagation and product production to perform multiple complex chemical conversions in a single unit operation. Previous studies conducted with *L. starkeyi* also demonstrated that harvesting cells after cell propagation in nitrogen-rich media and transferring the cells into nitrogen-free media for lipid production could effectively achieve high lipid productivity and a high conversion rate of carbon source to lipid. Therefore, our strategy is to separate the cell propagation and lipid production phases to maximize the lipid production (Figure 1). After maximizing cell number with nitrogen-rich medium (0.5 L of feeding medium containing 500 g L^{-1} glucose with a C/N = 16) by the exponential feeding from 52 to 68 h, we performed a preliminary experiment to estimate glucose consumption rate and lipid yield against glucose in the lipid production phase by only feeding nitrogen-free synthetic media. When 1 L of nitrogen-free synthetic media (no nitrogen source) containing 500 g L^{-1} glucose was added after exponential feeding, the glucose consumption rate and lipid yield were determined to be 30 g h^{-1} and 0.14 g g^{-1}, respectively (data not shown). To achieve a lipid titer comparable to the highest value of 68 g L^{-1} achieved in *L. starkeyi* using nutrient media [17], we calculated the expected glucose amount needed for reaching the previous value. Next, we determined to feed 3 L of feeding media (500 g L^{-1}) for lipid production. To prevent the overflow of culture media in the fermenter, we removed 1.5 L of cultures twice during lipid production (Figure 1 and Figure 5A). The residual glucose concentration was controlled to be lower than 20 g L^{-1} during lipid production in our study. The lipid titer and content reached 72 g L^{-1} and 61 % of DCW, respectively, by feeding nitrogen-free media (Figure 5A and Table 1). Although the titer was comparable to the reported data (68 g L^{-1}) [17], the cell titer (DCW) remained at a similar level from 127 to 195 h, with a decreasing cell density from 297 ± 19 to 120 ± 21 × 10^7 cells mL^{-1} (Figure 5A). Therefore, we considered that maintaining a sustained cell density during lipid production could further increase the lipid titer. We hypothesized that the addition of a trace amount of nitrogen would help cells to maintain the proper intracellular physiology for cell survival during lipid production phase. To confirm this concept, we supplemented nitrogen in the feeding media (C/N = 200 and 400). The results showed that the cell densities of C/N equal to 200 and 400 at the end of feeding (232 ± 35 and 178 ± 32 × 10^7 cells mL^{-1}) were higher than those of the nitrogen-free medium (120 ± 21 × 10^7 cells mL^{-1}) (Table 1). In addition, the lipid titers (88 ± 6 g L^{-1} for C/N equal to 200; 81 ± 5 g L^{-1} for C/N equal to 400) were higher than those achieved with the nitrogen-free medium (Table 1). As a result, the supplementation of a trace amount of nitrogen source during the lipid production phase could increase cell density and further elevate the lipid titer without ceasing lipid accumulation by *L. starkeyi*. Furthermore, we observed that the high cell density in the nitrogen-supplemented conditions shortened the cultivation time by consuming more glucose, leading to better lipid productivities and lipid yields in the whole

TABLE 1 | Cell number, DCW, and lipid production of *L. starkeyi* NBRC10381 fed by different molar C/N ratios during lipid production phase.

C/N ratio	Cultivation time h	MCD (maximum) [a] × 10^7 cells mL^{-1}	CD (final) [b] × 10^7 cells mL^{-1}	DCW [c] g L^{-1}	P_{titer} [d] g L^{-1}	$P_{content}$ [d] % (of DCW)	$Y_{P/S\ (whole)}$ [e] g g^{-1}	$R_{P\ (whole)}$ [e] g L^{-1} h^{-1}	$Y_{P/S\ (lipid)}$ [f] g g^{-1}	$R_{P\ (lipid)}$ [f] g L^{-1} h^{-1}
Nitrogen-free	197	413 ± 18	120 ± 21	118 ± 2	72 ± 4	61 ± 3	0.15 ± 0.00	0.16 ± 0.01	0.17 ± 0.00	0.37 ± 0.01
200	175	465 ± 63	232 ± 35	130 ± 5	88 ± 6	68 ± 2	0.17 ± 0.01	0.33 ± 0.02	0.19 ± 0.02	0.55 ± 0.03
400	175	505 ± 50	178 ± 32	145 ± 6	81 ± 5	56 ± 1	0.16 ± 0.01	0.29 ± 0.01	0.18 ± 0.01	0.46 ± 0.02

Note: All experiments were carried out in parallel triplicates. Data are presented as mean ± standard deviation.

[a] $MCD_{(maximum)}$: maximum cell density during lipid production.

[b] $CD_{(final)}$: cell density at the end of cultivation.

[c] DCW: dry cellular biomass at the end of cultivation.

[d] P_{titer} and $P_{content}$: lipid titer and content at the end of cultivation.

[e] $Y_{P/S\ (whole)}$ and $R_{P\ (whole)}$: overall lipid yield and production rate during whole cultivation.

[f] $Y_{P/S\ (lipid)}$ and $R_{P\ (lipid)}$: lipid yield and production rate during the lipid production phase.

TABLE 2 | Comparison of biomass and lipid production of oleaginous microbes cultivated by various strategies using sugar-based media.

Strain	Medium and method	Scale (L)[a]	Cultivation time (h)	DCW (g L^{-1})[b]	$P_{content}$ (% of DCW)[c]	P_{titer} (g L^{-1})[c]	$Y_{P/S\ (whole)}$ (g g^{-1})[d]	$R_{P\ (whole)}$ (g L^{-1} h^{-1})[d]	Ref.
Cryptococcus albidus	Glucose, synthetic medium, two-stage cell recycling continuous fed-batch	1	192	20	56	11	0.32	0.57	[35]
C. curvatus	Glucose, nutrient medium, fed-batch (pulse-fed)	30	185	104	83	87[e]	0.25	0.47	[36]
Candida viswanathii	Glucose, nutrient medium, two-stage fed-batch (pulse-fed)	7	196	21	50	11	0.11[e]	0.05[e]	[37]
L. starkeyi	Glucose and xylose, nutrient medium, repeated fed-batch	3	237	85	49	42	0.10	0.18	[38]
L. starkeyi	Glucose, nutrient medium, fed-batch (pulse-fed) (pulse-fed maintain always >20 g L^{-1} of residual glucose	3	200	110	58	80	ND	0.40	[18]
L. starkeyi	Glucose, synthetic medium, two-stage fed-batch	5	175	130	68	88	0.19	0.33	This study
L. starkeyi	Glucose, nutrient medium, two-stage batch (cells were propagated at 15-L vessel and transfer to 7-L vessel for lipid production)	10, 7	80	97	66	64	0.23[e]	0.55	[39]
L. starkeyi	Glucose, nutrient medium, two-stage batch (cells were propagated at 15-L vessel and transfer to 7-L vessel for lipid production)	15, 7	70	104	65	68	0.23[e]	0.97[e]	[17]
R. toruloides	Glucose, nutrient medium, two-stage fed-batch (pulse-fed).	3.5	272	37	65	24	0.21	0.09	[40]
R. toruloides	Glucose, nutrient medium, two-stage fed-batch (pulse-fed maintain always ≤20 g L^{-1} of residual glucose	15	134	106	68	72[e]	0.23	0.54	[41]
R. toruloides	Glucose, nutrient medium, fed-batch (maintain residual glucose at 5 g L^{-1})	15	144	127	62	79	0.23	0.57	[42]

Abbreviation: ND, no data.

[a]All bioreactors reported in Table 2 are stirred tank unless specified.

[b]DCW: dry cellular biomass at the end of cultivation.

[c]$P_{content}$ (% of DCW) and P_{titer} (g L^{-1}): lipid titer and content at the end of cultivation.

[d]$Y_{P/S\ (whole)}$ (g g^{-1}) and $R_{P\ (whole)}$ (g L^{-1} h^{-1}): overall lipid yield and production rate during whole cultivation.

[e]Calculated number according to the data from reference.

fermentation process or lipid production phases than those fed with nitrogen-free media (Table 2).

It is worth noting that despite similar levels of cell density during the cultivations, we observed higher lipid production (titer, content, yield, and productivity) when employing a molar C/N ratio of 200 as compared to molar C/N ratio of 400 (Table 1). Several reasons were considered. First, we suspected that the overshoot of glucose at 79 h may be the cause. A previous study demonstrated that controlling the residual glucose concentration to be lower than 5 g L^{-1} throughout the lipid production phase could increase lipid titer up to 1.4 times higher than that achieved while maintaining glucose concentration at 30 g L^{-1} in *Rhodosporidium toruloides* [42]. The amount of nitrogen used for the biosynthesis of microbial lipids may be another cause. Although nitrogen depletion triggers lipid accumulation in oleaginous yeasts, the cells still require a nitrogen source to produce enzymes and cofactors necessary for maintaining the cell survival [43]. One study showed that fresh medium with nitrogen sources can be applied to restart an exponential cell propagation process and further boost lipid production in repeated fed-batch cultures [42]. Therefore, we considered that the supplementation of a trace amount of nitrogen could also help the cells retain the intracellular physiology during lipid production.

Additionally, we observed that the residual phosphate concentration during the lipid production phase gradually accumulated in the culture media as the cell density reached its highest levels during the cultivation process. The lowest residual phosphate concentration was reached when the maximum cell density was achieved in all culture conditions (Figure 5). Subsequently, the cell density gradually decreased with an increment of phosphate accumulation. The data implied that the phosphate demand was different for cell growth and lipid production. Wierzchowska et al. [44] demonstrated that phosphate could increase biomass for producing lipids in oleaginous yeast *Yarrowia lipolytica*. The group suggested that determining the correlation between N/P molar ratio, biomass growth, and efficient lipid accumulation is crucial. Taken together, the phosphate demand in different phases could further be investigated and optimized in the future in *L. starkeyi*. Comparing our data with previous studies that used sugar-based (glucose and xylose) nutrient media or synthetic media for lipid production in oleaginous yeasts (Table 2), our study achieved the highest biomass (130 g L^{-1}) and lipid titer (88% of DCW) among early studies.

3.4 | *L. starkeyi* Microbial Lipids Mainly Composed of Oleic Acid and Palmitic Acid and Are Not Affected by Different Nitrogen Content in the Medium

The microbial lipids produced by *L. starkeyi* are known to mainly contain 14–18 carbons and exhibit low degrees of unsaturation, which are similar to palm oils [38]. To confirm the fatty acid profiles of the lipids produced in this study, the lipids produced by feeding media with different molar C/N ratios were transmethylated and analyzed by gas chromatography. The fatty acid profiles of the lipids mainly consist of palmitic acid (C16:0, comprising 28%–33% of total fatty acids) and oleic acid (C18:1, comprising 40%–42% of total fatty acids) (Figure 6), which is similar to other reports [28]. Although fatty acid profiles can differ when culture conditions change in oleaginous microbes [44], there were no significant differences observed in the fatty acid profiles between the different culture conditions (Figure 6). Taken together, the lipids produced using the method we demonstrated have the potential to serve as a palm oil–like feedstock for industrial applications.

4 | Conclusions

The present data have demonstrated a novel two-phase feeding strategy with synthetic media that separates the high-cell-density growth phase from the lipid production phase. By supplying a trace concentration of nitrogen during the lipid production phase, a high cell density could be sustained without ceasing lipid production by the cells, enabling a non-engineered *L. starkeyi* strain to achieve a comparable lipid titer (88 g L^{-1}) and a high biomass (130 ± 5 g L^{-1}) as those in a nutrient medium. To the best of our knowledge, this represents the highest reported lipid titer and biomass among all *L. starkeyi* studies to date. This observation highlights the importance of well-established yet powerful biochemical engineering approaches for the precise control of microbial cultivation, which is crucial for chemical manufacturing. In addition, the data also demonstrate the importance of phosphate in cell growth and the induction of lipid production of *L. starkeyi*. We believe that this method is not limited to just *L. starkeyi* but can also be applied in processes aimed at converting inexpensive and renewable materials into lipids and related products in the future.

Author Contributions

Chih-Chan Wu: writing–original draft, investigation. **Kenji Okano:** writing–review and editing, methodology. **Religia Pijar:** investigation. **Yuki Soma:** investigation. **Masatomo Takahashi:** investigation. **Yoshihiro Izumi:** writing–review and editing. **Takeshi Bamba:** writing–review and editing. **Kohsuke Honda:** conceptualization, supervision, writing–review and editing.

Acknowledgments

This paper is based on results obtained from a project, JPNP20011, commissioned by the New Energy and Industrial Technology Development Organization (NEDO). The authors greatly acknowledge the research grants provided by the NEDO Project (project code: P20011) of the Ministry of Economy, Trade, and Industry (METI), Japan, for this study.

Conflicts of Interest

The authors declare no conflicts of interest.

Data Availability Statement

Data will be made available on request.

References

1. C. R. Soccol, B. S. O. Colonia, G. V. de Melo Pereira, et al., "Bioprospecting Lipid-Producing Microorganisms: From Metagenomic-Assisted Isolation Techniques to Industrial Application and Innovations," *Bioresource Technology* 346 (2022): 126455.

2. J. Wang, S. D. Singer, B. A. Souto, et al., "Current Progress in Lipid-Based Biofuels: Feedstocks and Production Technologies," *Bioresource Technology* 351 (2022): 127020.

3. P. Szczepańska, P. Hapeta, and Z. Lazar, "Advances in Production of High-Value Lipids by Oleaginous Yeasts," *Critical Reviews in Biotechnology* 42 (2022): 1–22.

4. E. E. Karamerou and C. Webb, "Cultivation Modes for Microbial Oil Production Using Oleaginous Yeasts—A Review," *Biochemical Engineering Journal* 151 (2019): 107322.

5. A. B. Juanssilfero, P. Kahar, R. L. Amza, et al., "Effect of Inoculum Size on Single-Cell Oil Production From Glucose and Xylose Using Oleaginous Yeast *Lipomyces starkeyi*," *Journal of Bioscience and Bioengineering* 125 (2018): 695–702.

6. J. Brandenburg, J. Blomqvist, J. Pickova, N. Bonturi, M. Sandgren, and V. Passoth, "Lipid Production From Hemicellulose With *Lipomyces starkeyi* in a pH Regulated Fed-Batch Cultivation," *Yeast* 33 (2016): 451–462.

7. C. H. Calvey, Y. K. Su, L. B. Willis, M. McGee, and T. W. Jeffries, "Nitrogen Limitation, Oxygen Limitation, and Lipid Accumulation in *Lipomyces starkeyi*," *Bioresource Technology* 200 (2016): 780–788.

8. W. Zhou, Y. Wang, J. Zhang, et al., "A Metabolic Model of *Lipomyces starkeyi* for Predicting Lipogenesis Potential From Diverse Low-Cost Substrates," *Biotechnology for Biofuels* 14 (2021): 148.

9. M. C. A. Xavier, A. L. V. Coradini, A. C. Deckmann, and T. T. Franco, "Lipid Production From Hemicellulose Hydrolysate and Acetic Acid by *Lipomyces starkeyi* and the Ability of Yeast to Metabolize Inhibitors," *Biochemical Engineering Journal* 118 (2017): 11–19.

10. J. Zhang, Y. Wang, Q. Gou, et al., "Consolidated Bioprocessing of Cassava Starch Into Microbial Lipid for Biodiesel Production by the Amylolytic Yeast *Lipomyces starkeyi*," *Industrial Crops and Products* 177 (2022): 114534.

11. L. Liu, M. Zong, Y. Hu, N. Li, W. Y. Lou, and H. Wu, "Efficient Microbial Oil Production on Crude Glycerol by *Lipomyces starkeyi* AS 2.1560 and Its Kinetics," *Process Biochemistry* 58 (2017): 230–238.

12. R. Riley, S. Haridas, K. H. Wolfe, et al., "Comparative Genomics of Biotechnologically Important Yeasts," *Proceedings of the National Academy of Sciences of the United States of America* 113 (2016): 9882–9887.

13. H. Takaku, T. Matsuzawa, K. Yaoi, and H. Yamazaki, "Lipid Metabolism of the Oleaginous Yeast *Lipomyces starkeyi*," *Applied Microbiology and Biotechnology* 104 (2020): 6141–6148.

14. H. Takaku, A. Miyajima, H. Kazama, et al., "A Novel Electroporation Procedure for Highly Efficient Transformation of *Lipomyces starkeyi*," *Journal of Microbiological Methods* 169 (2020): 105816.

15. Y. Oguro, H. Yamazaki, S. Ara, et al., "Efficient Gene Targeting in Non-Homologous End-Joining-Deficient *Lipomyces starkeyi* Strains," *Current Genetics* 63 (2017): 751–763.

16. S. S. Tchakouteu, O. Kalantzi, C. Gardeli, A. A. Koutinas, G. Aggelis, and S. Papanikolaou, "Lipid Production by Yeasts Growing on Biodiesel-Derived Crude Glycerol: Strain Selection and Impact of Substrate Concentration on the Fermentation Efficiency," *Journal of Applied Microbiology* 118 (2015): 911–927.

17. J. Lin, H. Shen, H. Tan, et al., "Lipid Production by *Lipomyces starkeyi* Cells in Glucose Solution Without Auxiliary Nutrients," *Journal of Biotechnology* 152 (2011): 184–188.

18. S. Tsakona, N. Kopsahelis, A. Chatzifragkou, S. Papanikolaou, I. K. Kookos, and A. A. Koutinas, "Formulation of Fermentation Media From Flour-Rich Waste Streams for Microbial Lipid Production by *Lipomyces starkeyi*," *Journal of Biotechnology* 189 (2014): 36–45.

19. P. Yang, Y. Chen, and D. A. Gong, "Development of a Defined Medium for *Corynebacterium glutamicum* Using Urea as Nitrogen Source," *3 Biotech* 11 (2021): 405.

20. B. Hahn-Hägerdal, K. Karhumaa, C. U. Larsson, M. Gorwa-Grauslund, J. Görgens, and W. H. van Zyl, "Role of Cultivation Media in the Development of Yeast Strains for Large Scale Industrial Use," *Microbial Cell Factories* 4 (2005): 31.

21. K. R. Pomraning, J. R. Collett, J. Kim, et al., "Transcriptomic Analysis of the Oleaginous Yeast *Lipomyces starkeyi* During Lipid Accumulation on Enzymatically Treated Corn Stover Hydrolysate," *Biotechnology for Biofuels* 12 (2019): 162.

22. L. Matsakas, A. A. Sterioti, U. Rova, and P. Christakopoulos, "Use of Dried Sweet Sorghum for the Efficient Production of Lipids by the Yeast *Lipomyces starkeyi* CBS 1807," *Industrial Crops and Products* 62 (2014): 367–372.

23. M. Koller, "A Review on Established and Emerging Fermentation Schemes for Microbial Production of Polyhydroxyalkanoate (PHA) Biopolyesters," *Fermentation* 4 (2018): 30.

24. R. Poontawee and S. Limtong, "Feeding Strategies of Two-Stage Fed-Batch Cultivation Processes for Microbial Lipid Production From Sugarcane Top Hydrolysate and Crude Glycerol by the Oleaginous Red Yeast *Rhodosporidiobolus fluvialis*," *Microorganisms* 8 (2020): 151.

25. L. Liu, G. Du, J. Chen, M. Wang, and J. Sun, "Enhanced Hyaluronic Acid Production by a Two-Stage Culture Strategy Based on the Modeling of Batch and Fed-Batch Cultivation of *Streptococcus zooepidemicus*," *Bioresource Technology* 99 (2008): 8532–8536.

26. L. Mears, S. M. Stocks, G. Sin, and K. V. Gernaey, "A Review of Control Strategies for Manipulating the Feed Rate in Fed-Batch Fermentation Processes," *Journal of Biotechnology* 245 (2017): 34–46.

27. E. Bolmanis, K. Dubencovs, A. Suleiko, and J. Vanags, "Model Predictive Control—A Stand Out Among Competitors for Fed-Batch Fermentation Improvement," *Fermentation* 9 (2023): 206.

28. H. Takaku, S. Ebina, K. Kasuga, et al., "Isolation and Characterization of *Lipomyces starkeyi* Mutants With Greatly Increased Lipid Productivity Following UV Irradiation," *Journal of Bioscience and Bioengineering* 131 (2021): 613–621.

29. A. S. Hanner, M. Dunworth, R. A. Casero, C. W. MacDiarmid, and M. H. Park, "Elevation of Cellular Mg2+ Levels by the Mg2+ Transporter, Alr1, Supports Growth of Polyamine-Deficient *Saccharomyces cerevisiae* Cells," *Journal of Biological Chemistry* 294 (2019): 17131–17142.

30. F. Mollinedo, "Lipid Raft Involvement in Yeast Cell Growth and Death," *Frontiers in Oncology* 2 (2012): 140.

31. T. Kimura, Y. Mayumi, M. Takeuchi, K. Hayashi, and E. Ichishima, "Substrate Specificity of Carboxyl Proteinase of *Aspergillus sojae*," *Current Microbiology* 3 (1979): 153–156.

32. S. Wu, C. Hu, G. Jin, X. Zhao, and Z. K. Zhao, "Phosphate-Limitation Mediated Lipid Production by *Rhodosporidium toruloides*," *Bioresource Technology* 101 (2010): 6124–6129.

33. J. M. Burg, C. B. Cooper, Z. Ye, et al., "Large-Scale Bioprocess Competitiveness: The Potential of Dynamic Metabolic Control in Two-Stage Fermentations," *Current Opinion in Chemical Engineering* 14 (2016): 121–136.

34. S. Shioya, K. Shimizu, and T. Yoshida, "Knowledge-Based Design and Operation of Bioprocess Systems," *Journal of Bioscience and Bioengineering* 87 (1999): 261–266.

35. R. Fu, Q. Fei, L. Shang, C. J. Brigham, and H. N. Chang, "Enhanced Microbial Lipid Production by *Cryptococcus albidus* in the High-Cell-Density Continuous Cultivation With Membrane Cell Recycling and Two-Stage Nutrient Limitation," *Journal of Industrial Microbiology & Biotechnology* 45 (2018): 1045–1051.

36. J. Zhang, X. Fang, X.-L. Zhu, et al., "Microbial Lipid Production by the Oleaginous Yeast *Cryptococcus curvatus* O_3 Grown in Fed-Batch Culture," *Biomass and Bioenergy* 35 (2011): 1906–1911.

37. I. Ayadi, O. Kamoun, H. Trigui-Lahiani, et al., "Single Cell Oil Production From a Newly Isolated *Candida viswanathii* Y-E4 and Agro-

Industrial By-Products Valorization," *Journal of Industrial Microbiology & Biotechnology* 43 (2016): 901–914.

38. A. Anschau, M. C. A. Xavier, S. Hernalsteens, and T. T. Franco, "Effect of Feeding Strategies on Lipid Production by *Lipomyces starkeyi*," *Bioresource Technology* 157 (2014): 214–222.

39. J. Lin, S. Li, M. Sun, et al., "Microbial Lipid Production by Oleaginous Yeast in D-xylose Solution Using a Two-Stage Culture Mode," *RSC Advances* 4 (2014): 34944–34949.

40. S. S. Tchakouteu, N. Kopsahelis, A. Chatzifragkou, et al., "*Rhodosporidium toruloides* Cultivated in NaCl-Enriched Glucose-Based Media: Adaptation Dynamics and Lipid Production," *Engineering in Life Sciences* 17 (2017): 237–248.

41. Y. Li, Z. Zhao, and F. Bai, "High-Density Cultivation of Oleaginous Yeast *Rhodosporidium toruloides* Y4 in Fed-Batch Culture," *Enzyme and Microbial Technology* 41 (2007): 312–317.

42. X. Zhao, C. Hu, S. Wu, H. Shen, and Z. K. Zhao, "Lipid Production by *Rhodosporidium toruloides* Y4 Using Different Substrate Feeding Strategies," *Journal of Industrial Microbiology & Biotechnology* 38 (2011): 627–632.

43. I. Gientka, M. Wirkowska-Wojdyła, E. Ostrowska-Ligęza, et al., "Enhancing Red Yeast Biomass Yield and Lipid Biosynthesis by Using Waste Nitrogen Source by Glucose Fed-Batch at Low Temperature," *Microorganisms* 10 (2022): 1253.

44. K. Wierzchowska, B. Zieniuk, D. Nowak, and A. Fabiszewska, "Phosphorus and Nitrogen Limitation as a Part of the Strategy to Stimulate Microbial Lipid Biosynthesis," *Applied Sciences (Switzerland)* 11 (2021): 11819.

Supporting Information

Additional supporting information can be found online in the Supporting Information section.